Bulletin of the Seismological Society of America, Vol. 83, No. 1, pp. 38-52, February 1993

NON-DOUBLE-COUPLE EARTHQUAKES AT THE HENGILL-GRENSDALUR VOLCANIC COMPLEX, ICELAND: ARE THEY ARTIFACTS OF CRUSTAL HETEROGENEITY?

BY GILLIAN R. FOULGER AND BRUCE R. JULIAN

ABSTRACT

Earthquakes with anomalous non-double-couple (non-DC) mechanisms have been observed at many geothermal and volcanic areas, and possible physical explanations have been offered for them that involve tensile fracture caused by high fluid pressure or thermal contraction due to cooling. Nevertheless, the possible biasing effects of wave propagation in structurally complicated volcanic regions has made the identification of non-DC mechanisms as true source phenomena uncertain.

Non-DC earthquakes are common at the Hengill-Grensdalur volcanic complex in southwestern Iceland. Of 178 microearthquakes recorded by a 23-station network in the summer of 1981, 84, or 47%, have non-DC mechanisms, based on conventional interpretation of *P*-wave first motions using a one-dimensional crustal model. In this paper, we re-analyze the best constrained of these events by numerically tracing rays in a three-dimensional tomographically derived model of the crust. Computed positions of rays on the focal spheres change by as much as 35°, with the largest changes being caused by revision of focal depths. The number of earthquakes with clearly non-DC mechanisms remains large, however (56 out of 131 or 43%); the anomalous mechanisms are not artifacts of the mis-mapping of rays onto the focal sphere.

INTRODUCTION

Reports of earthquake radiation patterns inconsistent with double-couple (DC) source mechanisms have become increasingly common in the seismological literature (Klein *et al.*, 1977; Julian, 1983; Foulger and Long, 1984; Julian and Sipkin, 1985; Shimizu *et al.*, 1987; Foulger, 1988b; Foulger *et al.*, 1989). Many of these reports concern earthquakes in volcanic or geothermal areas, but the observations differ in detail. Departures from the classical quadrantal radiation pattern may be major or minor, the polarity fields may not be equal in size, and when they are unequal either compressions or dilatations may dominate. Such departures have traditionally been attributed to observational error or to anomalous wave-propagation effects, and solutions usually have been constrained *a priori* to be double couples. A growing body of high-quality data, however, supports the conclusion that non-DC mechanisms are true source phenomena and that these earthquakes are caused by some process other than simple shear slip on planar faults.

Well-constrained non-DC earthquakes are rare, and no completely satisfactory physical explanation for them has yet been found. Explanations that have been proposed include multiple simultaneous shear-slip events, slip on nonplanar faults, and motion perpendicular to faults (tensile faulting). Unbalanced compressional and dilatational fields imply a volume change at the source, which cannot be produced by any process that involves only shear faulting. Volume changes require some other process, such as a rapid phase change, the nearly instantaneous migration of material to or from the source volume, or the

presence of voids at depths in the Earth's crust where confining pressures exceed one kilobar. Before accepting any such interpretations of non-DC radiation patterns as source effects, we must rule out other explanations. These include the possibility that the anomalous mechanisms are artifacts of observational error or of seismic-wave propagation through regions of complex structure. Lateral inhomogeneities in crustal structure, if they are not adequately modeled, can distort the apparent radiation patterns from DC earthquakes and produce spurious non-DC components in inferred mechanisms.

Probably the best examples of non-DC earthquakes for test cases occur at the Hengill-Grensdalur volcanic complex in southwestern Iceland. The area contains a spreading plate boundary, three active volcanic systems, and an extensive high-temperature geothermal area currently under exploitation. It exhibits continuous microearthquake activity, which in 1981 was monitored by a 23-station seismometer network in an experiment aimed at geothermal prospecting (Foulger and Long, 1984; Foulger, 1988a, b). Many of the small earthquakes that were observed have predominantly explosive radiation patterns, as evidenced by the polarities of *P* waves. Foulger and Long (1984) and Foulger (1988b) interpreted the non-DC mechanisms as source effects and proposed that the earthquakes are caused by tensile cracking induced by thermal contraction of cooling rocks at the heat source of the geothermal area.

The detailed three-dimensional structure of the Hengill-Grensdalur area is known from a seismic tomography study that used arrival-time data from the 1981 experiment (Foulger and Toomey, 1989; Toomey and Foulger, 1989). This study resolved substantial lateral wave-speed variations in the roots of the volcanic complex, with the horizontal gradient even exceeding the vertical one in some places. As a by-product of the tomographic study, the earthquake hypocenters were recalculated using the three-dimensional crustal structure.

In this paper, we evalaute quantitatively the effect of complex structure on the focal mechanisms determined by Foulger and Long (1984) and Foulger (1988b). We apply numerical raytracing methods to the three-dimensional structure, using revised hypocentral estimates from the tomographic study, and compare the computed ray directions at the earthquake foci with those from the original study, which was based on a one-dimensional model. In a few cases, large changes in the estimated focal depths cause substantial systematic changes in take-off angles. The direct effects of crustal heterogeneity on the ray paths are smaller, however, and change ray directions at the focus by only a few degrees. The combined effects of hypocentral relocation and ray distortion cannot account for the non-DC radiation patterns for most of the well-constrained events. Non-DC source processes are necessary to explain the observations.

Non-DC Radiation Patterns

Seismologists usually assume that earthquakes are caused by shear slip on faults and that they therefore have DC source mechanisms and quadrantal compressional-wave radiation patterns. Most seismic data are consistent with this assumption, and most methods of routine analysis constrain focal mechanisms to be double couples. Data that are inconsistent with DC interpretations are generally, and often justifiably, attributed to experimental error. As seismometer networks have become denser and more sophisticated and seismic data have increased in quality, however, many earthquakes have been found

that are not adequately explained by the shear-slip theory. The fact that most of these reported non-DC earthquakes occur in volcanic and geothermal areas suggests that unusual physical effects, such as thermal stresses or the movement of high-pressure fluids, may play key roles in the source processes and that understanding them may lead to new insights about earthquakes and geothermal processes.

Two large (magnitude > 6) non-DC events occurred near Long Valley caldera, eastern California, in 1980 (Julian, 1983; Julian and Sipkin, 1985). They exhibit nearly pure "compensated linear-vector dipole" (CLVD) radiation patterns (Knopoff and Randall, 1970) and were interpreted as resulting from tensile failure on near-vertical surfaces. These earthquakes did not have significant volumetric components, and one had a complicated source-time function, so another possible explanation for them is complex rupture on more than one fault plane (Ekström, 1983; Wallace *et al.*, 1983). Many complex earthquakes with non-DC mechanisms may have such an explanation, and indeed moment-tensor inversion of long-period body waveforms can often resolve them into DC subevents (Sipkin, 1986). The Long Valley earthquakes, however, are unusual in having mechanisms with large and consistent non-DC components at all times.

Small explosive and implosive earthquakes occurred during a fissure eruption on Miyakejima Island, Japan, in 1983 (Shimizu *et al.*, 1987). Modeling of the compressional- and shear-wave amplitudes led to the conclusion that they were generated by simultaneous tensile and shear faulting, occurring in response to magnetic intrusion and withdrawal. A larger event with a magnitude of 3.2 and displaying predominantly compressional arrivals was observed at the Unzen Volcano, in southern Japan, in 1987, and a similar amplitude analysis showed that the direction of the T axis coincides with the extension direction of the graben. The event was attributed to fluid intrusion.

Several cases of non-DC events at the spreading plate boundary in Iceland are reported. Klein *et al.* (1977), while studying the Reykjanes spreading segment in southwestern Iceland, observed a large earthquake swarm in September 1972, which included small earthquakes with reduced dilatational fields. They suggested that these radiation patterns result from the distortion of ray paths by complex structure, though they also pointed out that a tensile-shear cracking model caused by rapid dike injection could account for the observations.

Many earthquakes with predominantly compressional first motions were observed by Foulger and Long (1984) and Foulger (1988b) at the Hengill-Grensdalur volcanic complex in southwestern Iceland. For 84 out of 178 events, compressional first motions cover most of the focal sphere, and the dilatational fields are severely reduced. The events were attributed to tensile cracking in the contracting rocks at the heat source of the geothermal area. Because a tensile crack has an entirely compressional P-wave radiation pattern, some other effect, such as simultaneous shear faulting or a rapid pore-pressure decrease, must produce the dilatational arrivals. These earthquakes and their geologic setting are discussed in more detail in the following sections, and the data from them are subjected to re-analysis using a three-dimensional model of crustal structure.

More recently, non-DC earthquakes have been reported from the Krafla spreading center in northeastern Iceland (Foulger *et al.*, 1989; Arnott, 1990).

Both explosive and implosive events were observed in the geothermal area and along the plate boundary and attributed to cracks opening and cavities collapsing in a heterogeneous stress field following a major dike injection episode.

Common factors in all the cases mentioned above are volcanic environments and suggestions of fluid movement and displacements perpendicular to the plane of fracture. The possibility of non-DC source processes should be borne in mind when studying volcanic and geothermal earthquakes, which involve source processes fundamentally different from those of tectonic earthquakes, and misidentification of event type may result in serious errors of interpretation.

Geothermal Seismicity at the Hengill-Grensdalur Volcanic Complex

The Hengill-Grensdalur volcanic complex forms part of the ridge-ridge-transform triple junction where the South Iceland Seismic Zone meets the mid-Atlantic Ridge in southwestern Iceland (Fig. 1). Three volcanic systems have been identified within it: the currently active Hengill system, the subsidiary Hromundartindur system, and the older Grensdalur system. These systems are discrete loci of crustal spreading or volcanism, and volcanic and tectonic activity has migrated between them during the last 1 Ma. Details of their structure and interrelationships are summarized by Foulger and Toomey (1989). All three systems have NNE-trending fissure swarms, postglacial lavas (younger than 10,000 years), and widespread high-temperature (> 200°C in the upper 1000 m) geothermal resources. The Hengill and Grensdalur systems contain central volcanoes. The South Iceland Seismic Zone, which represents the transform branch of the triple junction, lies to the south of the volcanic complex and contains low-temperature geothermal resources (< 150°C in the upper 1000 m).

Seismicity. The entire triple junction displays a continuous background of small-magnitude earthquakes (Foulger, 1988a) and has been spatially and temporally constant for at least 15 years. In the summer of 1981 a detailed study, described by Foulger (1988a, b), Toomey and Foulger (1989), and Foulger and Toomey (1989), was conducted, with the aim of using microearthquakes for geothermal prospecting (Foulger, 1982). A radio-telemetered network of 23 vertical 1-Hz seismometers recording on FM magnetic tape operated for 3 months and detected 2000 locatable earthquaks (Fig. 2). For 178 of these, well-constrained focal mechanisms were derived using *P*-wave polarities. Focal depths ranged from 2 to 7 km. The largest event recorded during the experiment had a local magnitude of 2.2.

Many of the earthquakes observed in 1981 have non-DC radiation patterns, with compressional first motions covering most of the focal sphere. Aside from their first-motion patterns, though, these earthquakes exhibit no obviously anomalous characteristics, as the typical seismograms in Figure 3 illustrate. Thus the Hengill non-DC earthquakes are not examples of "long-period events" (Fehler, 1983; Koyanagi *et al.*, 1987), "B-type earthquakes" (Minakami, 1974), or other types of volcanic-seismic events that are anomalous in duration, spectral character, or the partitioning of energy between compressional and shear waves.

The Hengill non-DC earthquakes were attributed by Foulger and Long (1984) and Foulger (1988b) to tensile crack formation within the heat source of the

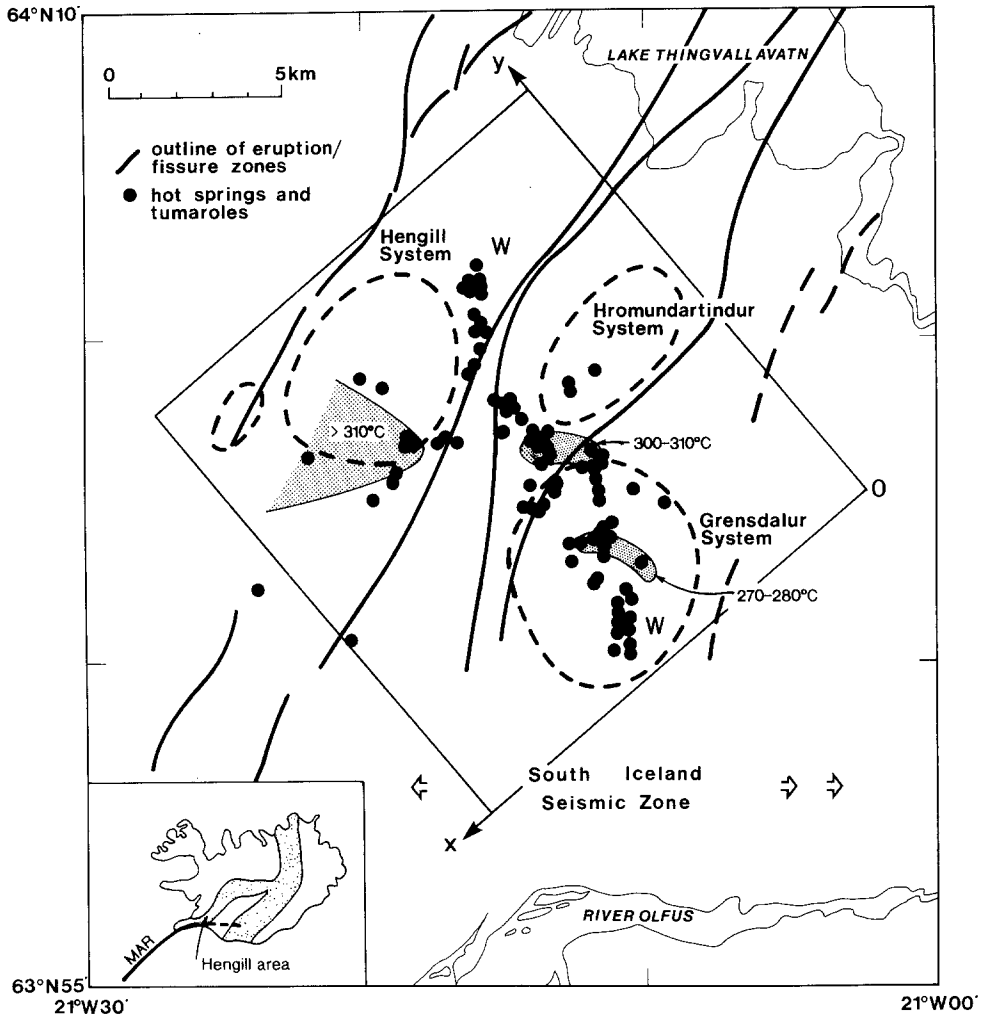

FIG. 1. Schematic tectonic map of the Hengill triple junction showing the three volcanic systems that have been identified. The central volcanoes within the Hengill and Grensdalur systems are outlined by dashed lines. Dots indicate hot springs and fumaroles. The three separate geothermal reservoir temperature maxima, determined from the geochemistry of fumarole gasses, are shaded. W indicates the two well fields. Large rectangle: location of tomographic crustal model of Toomey and Foulger (1989). The x axis has an azimuth of 230°. (Adapted from Saemundsson, 1967; Torfason *et al.*, 1983; Arnason *et al.*, 1986; Foulger, 1988a; Foulger and Toomey, 1989.) *Inset* shows the location of the Hengill triple junction in Iceland, with MAR = mid-Atlantic Ridge, and the neovolcanic zones on land in Iceland shaded.

geothermal area resulting from cooling contraction cracking. As mentioned above, however, tensile cracking alone cannot fully explain the seismological observations because in theory a pure tensile crack radiates compressive first motions in all directions (Aki and Richards, 1980, section 3.3), whereas the observed dilatational onsets, though uncommon, frequently are clear and unambiguous (Fig. 3).

Data Quality. Several kinds of seismometeric or seismological errors can produce data inconsistent with a DC focal-mechanism interpretation. These include

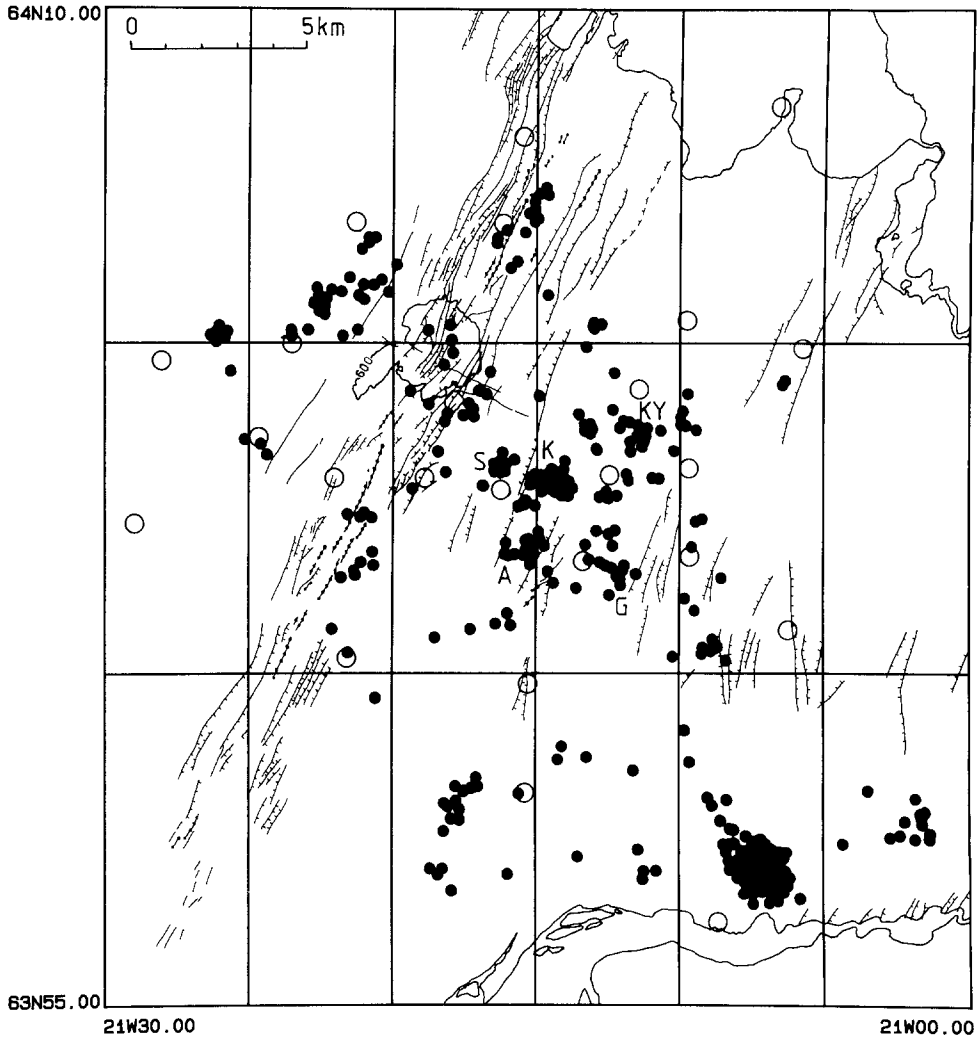

FIG. 2. Epicenters of the 843 best-located events recorded on the temporary radio-telemetered seismometer network during the three-month period from July to September 1981. Open circles indicate seismometer stations. Surface faults and fissures are indicated as lines. The clusters of activity referred to in Figure 5 are identified by letters. S = Svinahlid, A = Astadafjall, G = Grensdalur, K = Klambragil, KY = Kyllisfell.

errors in instrument polarity, calibration, or location, misidentification of seismic phases, and misreading of polarities on seismograms. For some types of data, such as those collected from heterogeneous instruments and observers and published in bulletins, or those from poorly maintained networks, sizeable error rates are to be expected.

The observations from the Hengill-Grensdalur area, however, cannot be attributed to errors in polarity determinations. The instruments were carefully calibrated in the laboratory both before and after the deployment, and the polarities were verified throughout the experiment by studying several well recorded explosions and teleseisms. In addition, only clear, impulsive first arrivals, for which the first motions are unambiguous, were used. Foulger and Long (1984), and Foulger (1988b) additionally argued against anomalous

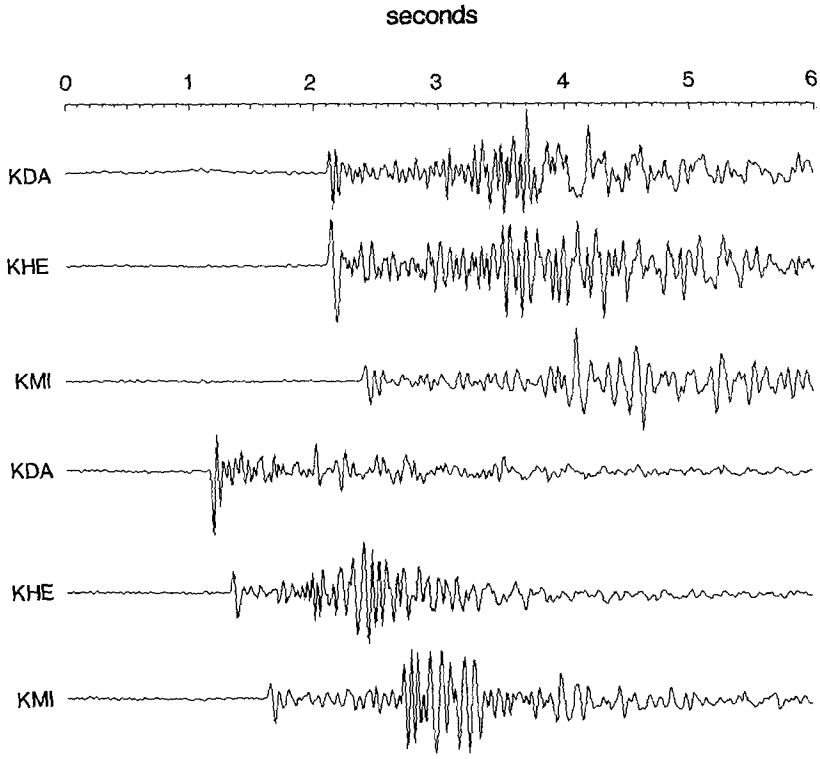

FIG. 3. Examples of typical seismograms from two Hengill-Grensdalur earthquakes recorded at three stations by Foulger and Long (1984). Top three traces: double-couple earthquake at 02:14 on 24 July 1981. Bottom three traces: non-DC earthquake at 22:58 on 31 July 1981.

propagation effects on the qualitative grounds that the DC and non-DC events are spatially mixed and must share similar propagation paths. They concluded that the only remaining explanation for the observations is a source effect.

Crustal Structure. The high-quality data set from the 1981 experiment was used in a later tomographic study (Foulger and Toomey, 1989; Toomey and Foulger, 1989). The *P*-wave arrival times were inverted, using the method of Thurber (1983), to refine the earthquake locations and to obtain a robust image of the upper 5 km of the crust. Considerable structure was discovered to be associated with the tripartite geothermal/volcanic complex. Bodies with compressional-wave speeds up to 15% higher than average and volumes of several tens of cubic kilometers exist beneath the Grensdalur volcano and the Hromundartindur system. These are probably largely solidified magma chambers that once fed the volcanic systems and now supply heat to the geothermal fields directly above. The Hengill volcano is underlain at depths of 2 to 4 km by a low-velocity body with a volume of a few cubic kilometers, which may contain partial melt.

EFFECTS OF THREE-DIMENSIONAL STRUCTURE

Unless it is properly accounted for, three-dimensional Earth structure introduces errors into first-motion focal mechanisms in two ways. First, unmodeled travel-time anomalies bias estimated hypocentral locations, causing errors, particularly in focal depths, that systematically distort the computed directions of seismic rays at the hypocenters. Second, variations in the wave speed perturb

the ray paths directly and produce similar, but generally less systematic, errors in computed ray directions. We assess these biasing effects quantitatively by numerically computing ray paths using the three-dimensional crustal model and the revised hypocenters of Toomey and Foulger (1989) and comparing the resulting ray directions with those used by Foulger and Long (1984), which were evaluated using a one-dimensional model.

Recomputation of the take-off angles was necessary because the tomographic software used by Toomey and Foulger (Thurber, 1983) does not use true raytracing, but rather an approximate technique, which selects from an *a priori* set of circular arcs the one that gives the smallest travel time. The use of such a path can give an adequate approximation to the correct travel time because the travel time is, to first order, stationary with respect to perturbation of the path away from the true ray (Fermat's Principle). Take-off angles, however, obey no such stationarity principle and require accurate ray paths for their evaluation.

Three-Dimensional Model. In their tomographic investigation, Toomey and Foulger (1989) used a right-handed Cartesian coordinate system with origin located at 64°2.48′ N, 21°2.20′ W, the z axis directed downward, and the x and y axes oriented in the directions 230° and 320° (Fig. 1). (Note that, because of constraints imposed by plotting software, the direction of the x axis is reversed in the figures of Toomey and Foulger (1989).) Values of the compressional-wave speed were specified at the nodes of a $8 \times 8 \times 7$ rectangular grid, $14 \times 15 \times 6$ km in dimensions, and oriented in the same way as the coordinate system. Additional nodes, at which the wave speed depends on depth only and is constrained during the inversion process, were placed on the planes $x = \pm 200$ km, $y = \pm 200$ km, and $z = \pm 50$ km. As discussed below, we move these outer nodes inward for our raytracing computations.

Figure 4b shows the compressional-wave speed in the model on a horizontal plane at 3-km depth, where lateral variations are strongest. The prominent high-speed anomaly near the middle of the region lies beneath the Hromundartindur system and is probably a solidified intrusion. The largest horizontal gradient in the model occurs on the northwest side of this body, where the wave speed decreases by about 1.5 km/sec over a distance of 2 km.

Raytracing. Computing the ray paths from the hypocenters to the stations is a two-point boundary-value problem, which we solve using the bending method (Julian and Gubbins, 1977), which iteratively perturbs an initial path (a straight line, here) until it satisfies the Euler equations that define a stationary-time path (ray).

The raytracing computations require values of the seismic-wave slowness (inverse of speed) and its spatial derivatives as functions of position, whereas the tomographic model consists of values of the wave speed at the nodes of a three-dimensional rectangular grid with variable spacing (Thurber, 1983; Thurber and Aki, 1987). The tomographic computations used trilinear interpolation between the nodes. This interpolation method is unsuitable for raytracing, because discontinuities in the gradient of the wave speed introduce discontinuities (shadow zones) into the ray field. To obtain values that vary smoothly, we use tri-cubic interpolation between the nodes. In this extension to three dimensions of the bicubic interpolation method described by Press *et al.* (1988), values of the seismic-wave slowness, s, and its spatial partial derivatives s_x, s_y, s_z,

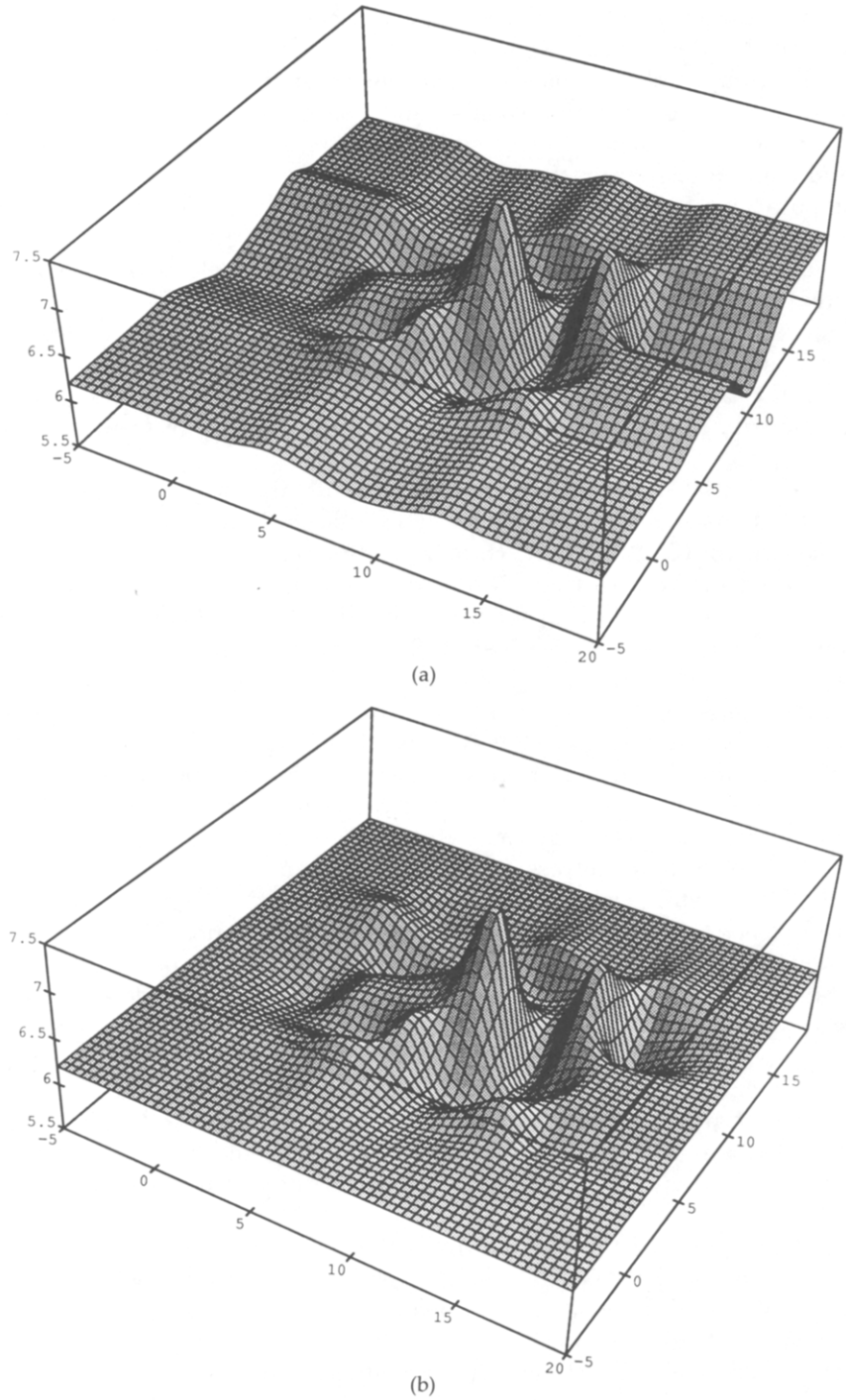

FIG. 4. Perspective view showing compressional-wave speed on horizontal plane at 3-km depth in crustal model for Hengill-Grensdalur area. Origin is at latitude 64°2.48′ N, Longitude 21°2.20′W. Positive x axis has an azimuth of 230°. View is from slightly east of north. See text for explanation of scheme used for interpolation between values at nodes of three-dimensional grid. (a) Values computed using original grid geometry of Toomey and Foulger (1989), which has bounding vertical planes at coordinates of $x = \pm 200$ km, $y = \pm 200$ km. Note the artificial and elongated anomalies outside the central region. (b) Values computed using modified grid geometry used in raytracing computations, with bounding vertical planes at $x = -5$ and 19 km, $y = -5$ and 20 km.

s_{xy}, s_{xz}, s_{yz}, and s_{xyz} are specified at the nodes and determine a unique tricubic polynomial in each grid block, with the slownesses and the above-mentioned derivatives automatically made continuous everywhere. The tomographic model gives the required slowness values directly, but not the partial derivatives. The method used here to determine values for the partial derivatives involves taking numerical differences of the slowness values at adjacent nodes. However, when combined with the usual practice in tomographic inversion studies of placing outer nodes on six planes at great distances from the others, the use of numerical-difference derivative values causes large and physically unrealistic fluctuations in the interpolated slownesses within the outermost grid blocks. To avoid this behavior, we set the normal derivatives to zero at the outer nodes and choose derivative values at the next-to-outermost nodes so that the interpolating polynomials are quadratic functions of distance from the boundaries and vary monotonically toward them.

Placing the outer nodes distant from the others has another unrealistic effect, which does not depend on the particular interpolation method used. This effect can be seen in Figure 4a. The elongated ridges and troughs parallel to the long axes of the outer blocks are artificial, and they introduce errors for computed rays that extend outside the central part of the model. This effect is small for the rays considered here, few of which extend far into the outermost grid blocks, but is severe for rays that travel to greater distances. We therefore use an altered grid spacing, placing the outer nodes on the planes $x = -5, +19$ km, $y = -5, +20$ km, and $z = -5, +11$ km, so that no dimension of any grid block exceeds 5 km. Outside the region bounded by these planes, the model is one dimensional. As Figure 4b shows, this change eliminates the artificial ridges and troughs.

The bending method of raytracing is iterative, and it can fail to converge, either when there is a shadow zone, so that no ray between the hypocenter and the station exists, or when the initial path is not close enough to the ray. For the three-dimensional model, about 8.5% of the rays fail to converge. Most of these failures probably are caused by shadow zones; for the one-dimensional model, which has no shadow zones, the failure rate is only about 1.5%.

In reanalyzing 140 of the best-constrained earthquakes from the 1981 experiment in the Hengill-Grensdalur area, we have traced more than 2000 rays through both the original one-dimensional model used by Foulger and Long (1984) and Foulger *et al.* (1989) and the three-dimensional model of Toomey and Foulger (1989). With 51 equally spaced points used to specify the path, computing a ray requires about 0.25 sec on a Sun SparcStation-I computer, illustrating that this type of analysis is practical on machines now in common use.

Results

Out of the total of 178 earthquakes originally analyzed by Foulger and Long (1984) and Foulger (1988b), we have re-analyzed the focal mechanisms of 131 using revised hypocentral locations and ray paths. A total of 47 earthquakes were excluded from re-analysis for two reasons: 28 because their locations are not well constrained and 19 because the number of rays that can be computed is insufficient.

Figure 5 shows, for 12 well-recorded earthquakes, the changes in computed ray directions that result from using the three-dimensional model and revised hypocenters. None of these earthquakes can be interpreted as DCs using directions corresponding to the one-dimensional model.

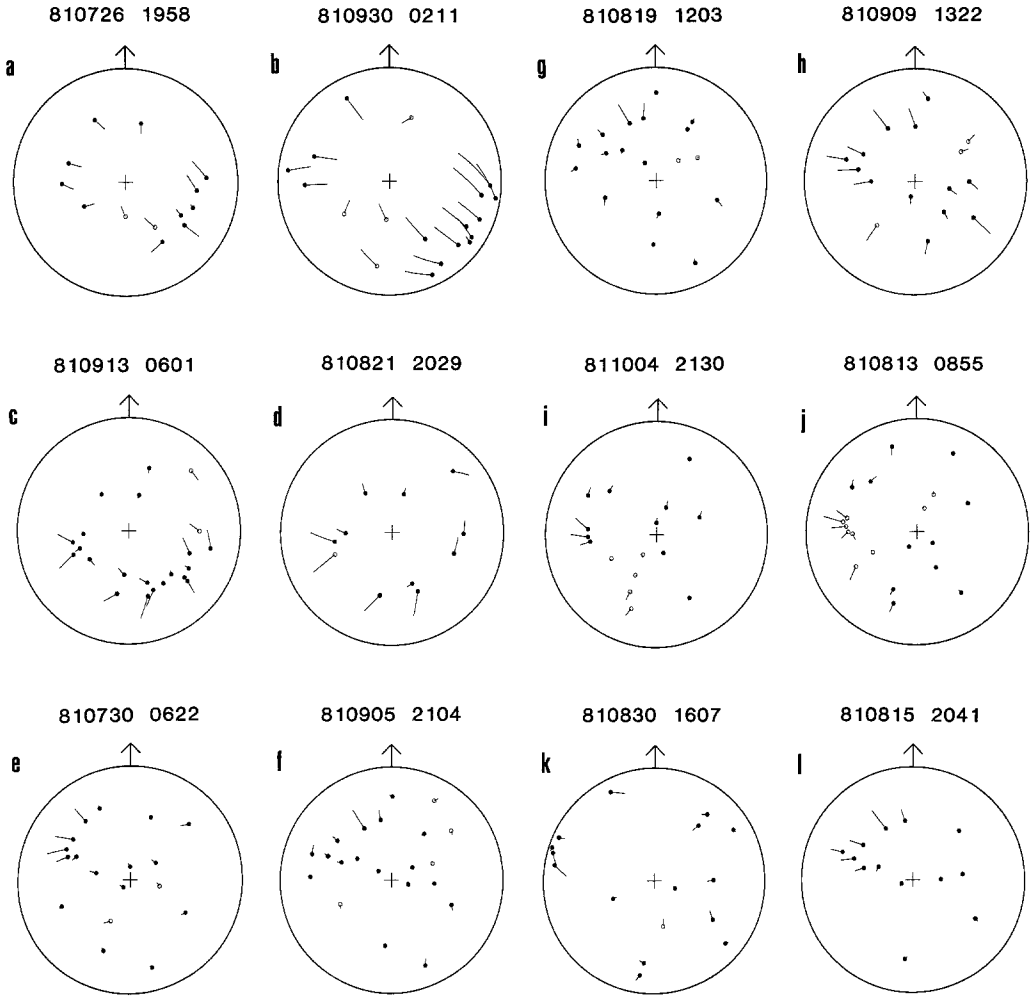

FIG. 5. Effect of three-dimensional structure on inferred directions of rays at hypocenters for 12 typical earthquakes. Upper focal hemispheres are shown in stereographic projection. Solid circles: compressions; open circles: rarefactions. Circles are plotted at ray directions computed by raytracing in three-dimensional model, using revised earthquake locations. Lines show changes from ray directions used by Foulger and Long (1984), which correspond to a one-dimensional crustal model.

Changes in focal depth cause the largest and most systematic changes in ray directions. Shallower depths correspond to smaller (i.e., more nearly downward) take-off angles and cause upward-departing rays to move toward the perimeters of the upper-hemisphere plots. This effect is most noticeable for the events of 810726 1958 and 810930 0211 (Figs. 5a and b), whose depths changed by $\Delta z = -0.89$ and -1.16 km. DC interpretations exist for the revised ray directions for these two earthquakes. The opposite effect, in which the focal depth and the take-off angles increase, is illustrated by the earthquake of 810821 2029 (Fig. 5d), for which $\Delta z = 0.53$ km. The ray positions move toward the center of the upper focal hemisphere, and DC interpretations remain impossible.

For most of the earthquakes, the revised depths are shallower, by amounts averaging about 0.3 km (Fig. 6), because the wave speeds are generally higher in the tomographic model. Figures 5c and (e) to (l) show nine well-recorded

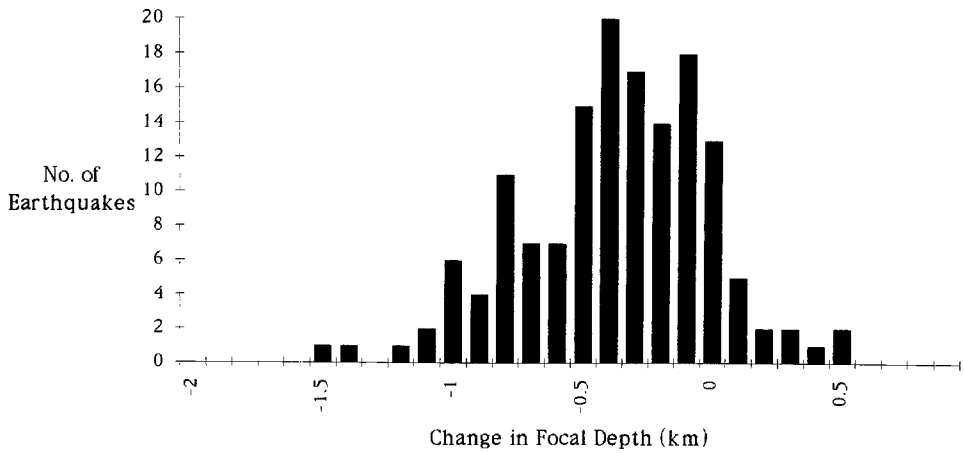

FIG. 6. Distribution of differences between focal depth estimates of Toomey and Foulger (1989), based on three-dimensional tomographic crustal model, and those of Foulger (1988a), based on one-dimensional model.

examples of these more typical events, for which Δz ranges from -0.41 to $+0.08$ km. The general outward motion of points caused by the decrease in average depth is not noticeable. Instead, the direct effects of three-dimensional anomalies dominate. Particularly noticeable are the effects of the high-speed region shown in Figure 4, which displace the directions of westward-departing rays (Figs. 5c, e, h, i, j, and l) and also cause clustering of rays on the western portion of the focal sphere.

Figure 7 shows stereoscopic views of the ray paths for four of the events whose focal-sphere plots are shown in Figure 5 and illustrates some of the effects mentioned above. The first two views (a and b) show rays from earthquakes in similar locations, but seen from different directions, and illustrate two effects: downward curvature of rays, which causes take-off angles computed from one-dimensional models to be biased toward smaller (more nearly downward) values, and spreading of rays with nearly the same departure directions so they emerge relatively far apart. This second effect causes stations in a large area to sample practically the same part of the focal sphere. Raytracing computations can be used to significantly improve the geometry of networks in such cases. The third view (c) is for an earthquake near the center of the model. This earthquake is relatively shallow (3 km), and its rays are not seriously distorted by three-dimensional structure. The last view (d) is for an earthquake northeast of the Hengill volcano and illustrates the downward bending of rays that propagate southward above the low-velocity region that underlies the volcano.

The behavior of the 12 examples shown in Figure 5 is typical of the total collection of 131 earthquakes whose focal mechanisms were re-analyzed. For 19 out of 73 earthquakes, changes in ray directions, caused primarily by revision of focal depths, make DC interpretations possible where they previously were not. For two events, the opposite occurs, and DC interpretations become impossible. But most significantly, there remain 56 well-constrained earthquakes whose first motions are incompatible with DC interpretations. The anomalous earthquake mechanisms from the Hengill-Grensdalur complex are not artifacts of complex crustal structure. Explanations for them must be sought in the physical processes acting at the source.

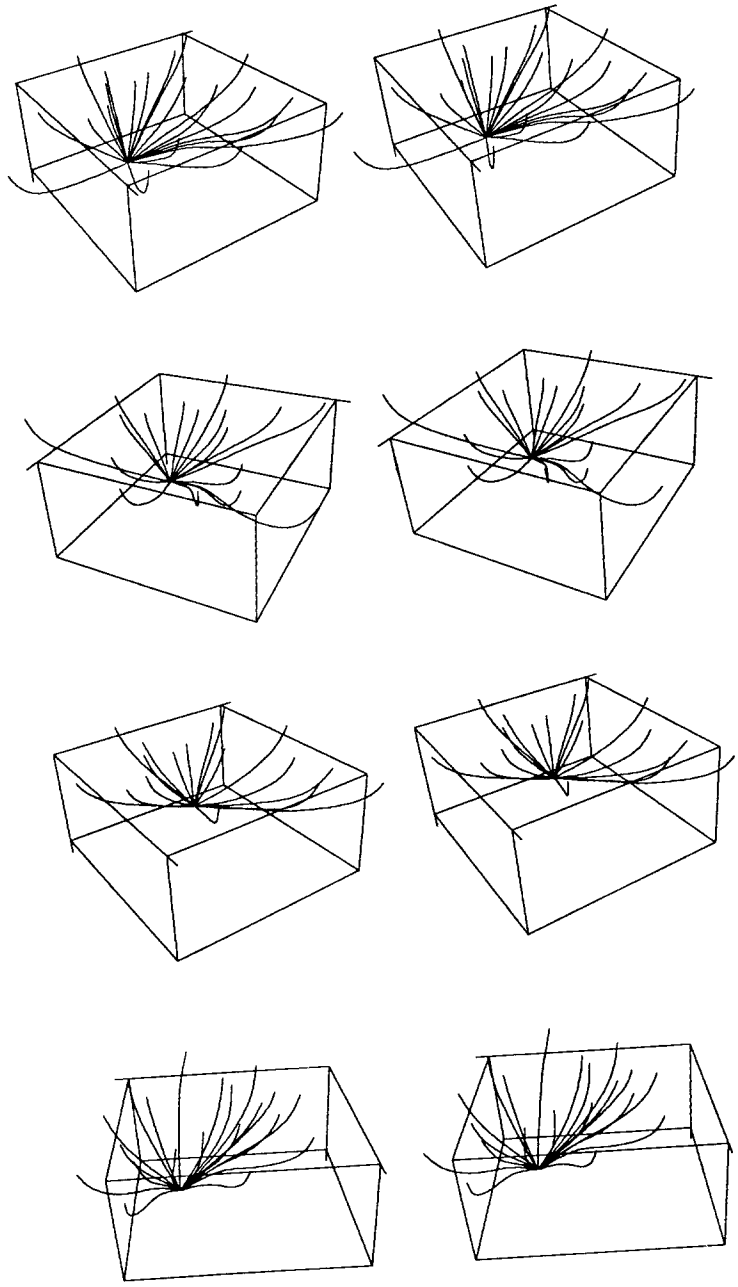

FIG. 7. Stereoscopic views of ray paths computed for P waves in three-dimensional model for four earthquakes. (a) Earthquake of 810813 0855 (Fig. 5j) at Kyllisfell (Fig. 2). View is toward S (azimuth 170°). Note downward curvature and clustering of take-off directions for rays departing toward the right (westward). (b) Earthquake of 811004 2130 (Fig. 5i) at Kyllisfell (Fig. 2). View is toward ESE (azimuth 110°). Note downward curvature, azimuth change, and clustering of take-off directions for rays departing toward the observer (westward). (c) Earthquake of 810830 1607 (Fig. 5k) at Klambragil (Fig. 2). View is toward S (azimuth 170°). Event is shallow (3 km), a few rays are strongly affected by lateral variations in crustal structure. (d) Earthquake of 810913 0601 (Fig. 5c) in the fissure swarm northeast of the Hengill volcano (Figs. 1 and 2). View is toward NE (azimuth 50°). Note downward curvature of many rays departing southward (toward observer).

CONCLUSIONS

1. Earthquakes exhibiting non-DC radiation patterns may be evidence of non-shear source processes, but before such an interpretation is accepted it is important to rigorously rule out other possible explanations for the observations.

2. Distortion of true earthquake radiation patterns can result from incorrect focal depths determined using an inaccurate crustal model. Additionally, where the velocity structure has a large three-dimensional component, significant distortion may arise if a one-dimensional model is used.

3. Non-DC radiation patterns are reported for many small earthquakes at the Hengill-Grensdalur volcanic complex, in southwestern Iceland. These were derived from first-motion polarities using a one-dimensional crustal model. We have critically re-analyzed 73 of these, and also 58 non-anomalous earthquakes, by correcting for the effects of errors in focal depths and three-dimensional crustal structure.

4. Changes in inferred ray directions at the sources are considerable and systematic for a few events with large errors in their hypocentral depths. Bias resulting from distortion of rays by three-dimensional variations in seismic-wave speed is minor and unsystematic.

5. After correction, a few more events can be fitted with DC mechanisms, but 56, or 43%, still cannot.

6. The non-DC radiation patterns of earthquakes recorded in 1981 at the Hengill-Grensdalur volcanic complex are not explained by inadequate modeling of the velocity structure.

7. Non-DC earthquakes at the Hengill-Grensdalur volcanic complex are evidence of source processes other than simple shear faulting.

ACKNOWLEDGMENTS

During this work, we had valuable discussions with Stuart Arnott. Andy Michael helped in preparing the focal-sphere plots of Figure 5. This research was supported partially by a grant from the Natural Environment Research Council and a G. K. Gilbert Fellowship from the U.S. Geological Survey.

REFERENCES

Aki, K. and P. G. Richards (1980). *Quantitative Seismology*, W. H. Freeman, San Francisco.

Arnason, K., G. I. Maraldsson, G. V. Johnsen, G. Thorbergsson, G. P. Hersir, K. Saemundsson, L. S. Georgsson and S. P. Snorrason (1986). Nesjavelliv, jardfraedi-og jardedlisfraedileg könnun 1985 (Nesjavellir, geological and geophysical investigations 1985). Nat. Energy Authority, Reykjavik, Report OS-86014/JHD-02.

Arnott, S. (1990). A seismological study of the Krafla volcanic system, Iceland, *Ph.D. Thesis*, University of Durham, Durham, United Kingdom.

Ekström, G. (1983). Evidence for source complexities of 1980 Mammoth Lakes earthquakes (abstract), *Eos* **64**, 769.

Fehler, M. (1983). Observations of volcanic tremor at Mount St. Helens volcano, *J. Geophys. Res.* **88**, 3476–3484.

Foulger, G. R. (1982). Geothermal exploration and reservoir monitoring using earthquakes and the passive seismic method, *Geothermics* **11**, 259–268.

Foulger, G. R. (1988a). The Hengill triple junction, SW Iceland. 1. Tectonic structure and the spatial and temporal distribution of local earthquakes, *J. Geophys. Res.* **93**, 13493–13506.

Foulger, G. R. (1988b). The Hengill triple junction, SW Iceland. 2. Anomalous earthquake focal mechanisms and implications for process within the geothermal reservoir and at accretionary plate boundaries, *J. Geophys. Res.* **93**, 13507–13523.

Foulger, G. R. and R. Long (1984). Anomalous focal mechanisms: tensile crack formation on an accreting plate boundary, *Nature* **310**, 43–45.

Foulger, G. R., R. E. Long, P. Einarsson, and A. Bjornsson (1989). Implosive earthquakes at the active accretionary plate boundary in northern Iceland, *Nature* **337**, 640–642.

Foulger, G. R. and D. R. Toomey (1989). Structure and evolution of the Hengill-Grensdalur volcanic complex, Iceland: Geology, geophysics, and seismic tomography, *J. Geophys. Res.* **94**, 17511–17522.

Hill, D. P. (1977). A model for earthquake swarms, *J. Geophys. Res.* **82**, 1347–1352.

Julian, B. R. (1983). Evidence for dyke intrusion earthquake mechanisms near Long Valley caldera, California, *Nature* **303**, 323–325.

Julian, B. R. and D. Gubbins (1977). Three-dimensional seismic ray tracing, *J. Geophys.* **43**, 95–113.

Julian, B. R. and S. A. Sipkin (1985). Earthquake processes in the Long Valley caldera area, California, *J. Geophys. Res.* **90**, 11155–11169.

Klein, F., P. Einarsson, and M. Wyss (1977). The Reykjanes Peninsula, Iceland, earthquake swarm of September 1972 and its tectonic significance, *J. Geophys. Res.* **82**, 865–888.

Knopoff, L. and M. J. Randall (1970). The compensated linear-vector dipole: a possible mechanism for deep earthquakes, *J. Geophys. Res.* **75**, 4957–4963.

Koyanagi, R. Y., B. Chouet, and K. Aki (1987). *Origin of volcanic tremor in Hawaii. Part I. Data from the Hawaiian Volcano Observatory 1969-1985, Volcanism in Hawaii, U.S. Geol. Surv. Profess. Pap. 1350*, R. W. Decker *et al.* (Editors), 1221–1259.

Minakami, T. (1974). Seismology of volcanoes in Japan, Physical Volcanology, *Developments in Solid Earth Geophysics*, Vol. 6, L. Civetta, P. Gasparini, G. Luongo, and A. Rapolla (Editors), Elsevier, Amsterdam, 1–27.

Press, W. A., B. P. Flannery, S. A. Teukolsky, and W. T. Vetterling (1988). *Numerical Recipes in C*, Cambridge University Press, New York.

Saemundsson, K. (1967). Vulkanismus und Tektonik des Hengill-Gebietes in Sudwest-Island. Acta Natur. Island, 2 (7), 109 pp.

Shimizu, H., S. Ueki, and J. Koyama (1987). A tensile-shear crack model for the mechanism of volcanic earthquakes, *Tectonophysics* **144**, 287–300.

Sipkin, S. A. (1986). Interpretation of non-double-couple earthquake mechanisms derived from moment tensor inversion, *J. Geophys. Res.* **91**, 531–547.

Thurber, C. H. (1983). Earthquake locations and three-dimensional crustal structure in the Coyote Lake area, central California, *J. Geophys. Res.* **88**, 8226–8236.

Thurber, C. H. and K. Aki (1987). Three-dimensional seismic imaging, *Ann. Rev. Earth Planet. Sci.* **15**, 115–139.

Toomey, D. R. and G. R. Foulger (1989). Tomographic inversion of local earthquake data from the Hengill-Grensdalur central volcano complex, Iceland, *J. Geophys. Res.* **94**, 17497–17510.

Torfason, H., G. P. Hersir, K. Saemundsson, G. V. Johnson and E. Gunnlangsson (1983). Vestur-Hengill. yfirbordsrannsokn jardhitasvaedisins. (West Hengill. Surface research of the geothermal field). Nat. Energy Authority, Reykjavik, Report OS-83119/JHD-22, 113 pp.

Wallace, T. C., L. J. Burdick, and H. Kanamori (1983). Faulting and crustal structure complexity: possible explanation for the moment tensor solutions of the 1980 Mammoth Lakes earthquakes (abstract), *Eos* **64**, 769.

DEPT. OF GEOLOGICAL SCIENCES
UNIVERSITY OF DURHAM
SCIENCE LABORATORIES, SOUTH ROAD
DURHAM DH1 3LE
UNITED KINGDOM
(G. R. F.)

U.S. GEOLOGICAL SURVEY
MS 977
345 MIDDLEFIELD ROAD
MENLO PARK, CALIFORNIA 94025
(B. R. J.)

Manuscript received 15 January 1992